

## Supporting Information

### **Defective S/N co-doped carbon cloth *via* a one-step process for effective electroreduction of nitrogen to ammonia**

**Shaoan Cheng,<sup>\*a</sup> Chaochao Li,<sup>a</sup> Zhen Yu,<sup>a</sup> Yi Sun,<sup>a</sup> Longxin Li<sup>a</sup> and Jiawei  
Yang<sup>a</sup>**

*State Key Laboratory of Clean Energy Utilization, College of Energy Engineering,  
Zhejiang University, Hangzhou, 310007, P.R.China*

*\*Corresponding author: Shaoan Cheng [shaoancheng@zju.edu.cn](mailto:shaoancheng@zju.edu.cn)*

## Experimental section

**Materials.** Acetone (Sinopharm Chemical Reagent Co., Ltd, C<sub>3</sub>H<sub>6</sub>O), isopropanol (Sinopharm Chemical Reagent Co., Ltd, C<sub>3</sub>H<sub>8</sub>O), ammonium persulfate (Aladdin, N<sub>2</sub>H<sub>8</sub>S<sub>2</sub>O<sub>8</sub>), sodium hydroxide (Sinopharm Chemical Reagent Co., Ltd, NaOH), salicylic acid (Aladdin, C<sub>7</sub>H<sub>6</sub>O<sub>3</sub>), trisodium citrate dihydrate (Aladdin, Na<sub>3</sub>C<sub>6</sub>H<sub>5</sub>O<sub>7</sub>·2H<sub>2</sub>O), sodium hypochlorite (Sinopharm Chemical Reagent Co., Ltd, NaClO), sodium nitroferricyanide(III) dihydrate (Aladdin, C<sub>5</sub>FeN<sub>6</sub>Na<sub>2</sub>O·2H<sub>2</sub>O), 4-dimethylaminobenzaldehyde (Aladdin, p-C<sub>9</sub>H<sub>11</sub>NO), sodium sulphate (Sinopharm Chemical Reagent Co., Ltd, Na<sub>2</sub>SO<sub>4</sub>), ammonium chloride (Aladdin, NH<sub>4</sub>Cl), hydrazine hydrate (Aladdin, N<sub>2</sub>H<sub>4</sub>·H<sub>2</sub>O), sulfuric acid (Sinopharm Chemical Reagent Co., Ltd, H<sub>2</sub>SO<sub>4</sub>, 98%), hydrochloric acid (Sinopharm Chemical Reagent Co., Ltd, HCl, 37%), ultrapure water (Aladdin, H<sub>2</sub>O), nitrogen gas (<sup>14</sup>N<sub>2</sub>, 99.999%; <sup>15</sup>N<sub>2</sub>, 99%, Sigma-Aldrich), and argon gas (Ar, 99.999%). The commercial carbon cloth (CC, HCP330N) was purchased from Shanghai HESEN company, which was composed of the interwoven carbon fibers and fabricated at high temperatures (1500~1800 °C) in Ar atmosphere. Nafion 117 was purchased from DuPont Co. Ltd and has been activated and purified before the experiments.<sup>1</sup> Before use, the N<sub>2</sub> gas was further purified by passing through 0.1 M KOH, 0.05 M H<sub>2</sub>SO<sub>4</sub>, and a Cu trap to remove the possible trace amount of NH<sub>3</sub> or NO<sub>x</sub>.<sup>2</sup>

**Preparation of the detective S/N codoped carbon cloth.** As shown in Fig. 1a, S/N codoped CC with abundant defects was prepared through a novel one-step

thermochemical method. In a typical preparation, commercial CC was clipped into strips (20 mm × 30 mm) and ultrasonically treated in acetone, isopropanol, alcohol, and ultrapure water for 10 min, respectively. 0.4 g as-cleaned CC was then stacked into a quartz boat and buried tightly in 2.4 g ground APS particles. The mixture should be stood in the air for 30 min for a slight deliquescence of APS. After that, the mixture was heated in a nitrogen-filled tube furnace at 170 °C for 30 min. This preheating procedure accelerates the melting of APS particles and subsequently form a covering layer on the surface of carbon fibers. Afterward, the APS-CC composite was heated to a certain degree of X (X=200, 400, 600, or 800 °C) with 5 °C/min and maintained for 2 h. The collected CCs were rinsed in alcohol and ultrapure water alternately for dozens of times and then dried at 80 °C for 8 h in a vacuum drying oven. The as-obtained catalyst was signed as CC-APS X (X represents the calcination temperature of 200, 400, 600, or 800 °C). The control sample of CC-800 was prepared by treating CC at 800 °C under similar conditions without APS.

***Structural characterizations.*** Thermal reaction characteristics of CC and APS were obtained by thermogravimetric analysis (TGA, TA-Q500, TA). The surface morphology and elemental distribution of CC catalysts were observed by scanning electron microscopy (SEM, S-4800, HITACHI) equipped with energy-dispersive X-ray spectroscopy (EDS). The microtopography and lattice properties were characterized by transmission electron microscopy (TEM, Tecnai G2 F20 S-Twin, FEI). The crystal structure was investigated through X-ray diffraction (XRD) patterns with Cu K $\alpha$  radiation ( $\lambda=1.5418$  Å, X'pert PRO, PANNAlytical). The elemental

chemical states of the CC-APS X were obtained by the X-ray photoelectron spectroscopic (XPS, XR3E2, Thermo scientific). The surface wettability was verified through contact angle tests (A-100P, Maist). Surface functional group distribution was analyzed through Fourier transform infrared spectroscopy (FTIR, AVA TAR370, NICOLET). The defects in CC-APS X were characterized by Raman spectra (LabRAM HR Evolution, Horiba Jobin Yvon). N<sub>2</sub> adsorption–desorption isotherms were obtained through N<sub>2</sub> absorption-desorption tests (3Flex, Micromeritics Instrument Ltd.). The specific surface area was calculated through the BET method. The pore size distribution of mesopores and micropores on the CC surface was calculated by BJH and NLDFT theory, respectively. The electrochemical active surface area (ECSA) of the catalysts was derived from a series of cyclic voltammetry (CV) curves by the electrochemical workstation (VMP3, Bio-Logic).<sup>3</sup> Temperature-programmed desorption (N<sub>2</sub>.TPD) of N<sub>2</sub> experiments were conducted on a Quantachrome ChemBET Pulsar TPR/TPD.<sup>4</sup> The <sup>1</sup>H NMR spectra were measured on an Ascend™ 400 Nuclear Magnetic Resonance Spectrometer.<sup>5</sup>

***Electrochemical measurements.*** The electrochemical tests of nitrogen reduction were executed in an H-type reactor with a typical three-electrode system.<sup>6</sup> During the experiment, the CC-APS X was clamped with a Pt electrode holder, leaving an exposing area of 0.5 cm × 1.0 cm in the electrolyte. The electrolyte solution is 100 mL aqueous solution composed of 0.05 M H<sub>2</sub>SO<sub>4</sub> and 0.2 M Na<sub>2</sub>SO<sub>4</sub>, showing a pH of 1.0 and a conductivity of 29.27 mS cm<sup>-1</sup>. The catalyst was used as the working electrode, coupling with the counter electrode of a graphite rod and Ag/AgCl

reference electrode. All the potentials during the tests were converted to the reversible hydrogen electrode (RHE) with  $E_{\text{RHE}} = E_{\text{Ag/AgCl}} + 0.256 \text{ V}$ . The anode and cathode chambers were separated by the proton exchange membrane (Nafion 117, DuPont Co. Ltd). Between different experiment cycles, the membrane would be re-activated and cleaned carefully.<sup>7</sup> The gas bubbling was controlled through a gas flowmeter, and the flow rate was controlled at  $30 \text{ mL min}^{-1}$ . All the experiments were repeated triply under mild temperature ( $30 \text{ }^\circ\text{C}$ ) and pressure ( $1.0 \text{ atm.}$ ), and the average values were accepted as reliable data. During the test, the reaction system has been well sealed during the tests to avoid the dissolution of the  $\text{NH}_3$  existing in the air ( $0.05\text{--}250 \text{ ppm}$ ) or the human breath ( $0.3\text{--}3.0 \text{ ppm}$ ).<sup>8</sup>

The dynamic electrochemical properties of the samples were measured by linear sweep voltammetry (LSV) tests with a scanning range of  $0.25 \sim -0.85 \text{ V vs. RHE}$  and a scanning rate of  $5 \text{ mV/s}$ . NRR performance of different catalysts at different applied potentials was tested by the chronoamperometry method. The long-term and cyclic electrolysis of CC-APS X was executed to confirm the stability of the catalysts. The electrochemical resistances of the resultant samples were measured through the electrochemical impedance spectroscopy (EIS) measurement at  $-0.3 \text{ V vs. RHE}$  for analyzing the electrochemical kinetics on the electrodes. The test frequency was in the range from  $1 \text{ MHz}$  to  $1 \text{ mHz}$ , and the amplitude was controlled at  $10 \text{ mV}$ . Before and during the electrolysis, high-pure  $\text{N}_2$  or  $\text{Ar}$  was continuously bubbled into the electrolyte solution with a rate of  $30 \text{ mL/min}$  under the control of the gas flowmeter. The electrochemical in situ FTIR spectra were carried out through the electrochemical

in situ spectrophotometer (Nexus 870, Thermo Fisher) to analyze the changes in the functional groups on the CC surface during the NRR process.

**Determination of  $NH_3$ .** The concentration of  $NH_3$  in the catholyte was quantitatively determined by an indophenol blue method.<sup>2</sup> Briefly speaking, the electrolyte solution after NRR test (2 mL) was mixed with NaOH (2 mL, containing 1 M NaOH, 5 wt.% salicylic acid and 5 wt.% sodium citrate), NaClO (1 mL, 0.05 M) and  $C_5FeN_6Na_2O$  (0.2 mL, 1 wt%) through a vigorous shake. After standing in the dark for 2 h, the absorption spectra of the electrolyte solution were measured by the UV-vis spectrophotometer (N6000 Plus, YOKE). The concentration of the generated  $NH_3$  was determined by the absorbance value at a wavelength of 655 nm. The  $NH_3$  concentration is calibrated by measuring the absorbance values of a series of standard  $(NH_4)_2SO_4$  solutions (**Fig. S7**). The  $NH_3$  yield and the FE is calculated with the following equations:

$$r_{NH_3} = \frac{c_{NH_3} \times V}{t \times A} \quad (S1)$$

$$FE = \frac{3F \times n_{NH_3}}{Q} \quad (S2)$$

where  $c_{NH_3} (mg L^{-1})$  is the measured concentration of  $NH_3$  in the electrolyte,  $V$  (mL) is the volume of the electrolyte,  $t$ (h) is the electroreduction time,  $A$  ( $cm^2$ ) is the surface area of the CC,  $F$  ( $96,485 C mol^{-1}$ ) is the Faraday constant,  $n_{NH_3} (mol)$  is the molar weight of the produced  $NH_3$ , and  $Q(C)$  is the total electricity consumption during the NRR process.

**Determination of  $N_2H_4$ .** The  $N_2H_4$  concentration in the electrolyte was quantitatively

determined by the method of Watt & Chrisp.<sup>2</sup> Briefly speaking, a mixture of 5.99 g p-C<sub>9</sub>H<sub>11</sub>NO, 30 mL HCl and 300 mL alcohol is prepared as the color reagent. Then, the electrolyte solution after electrolysis (5 mL) and the color reagent (5 mL) were thoroughly mixed with vigorous shaking. After standing in the dark for 15 min, the absorption spectra of the electrolyte solution were measured by the UV-vis spectrophotometer. The concentration of the generated N<sub>2</sub>H<sub>4</sub> was determined by the absorbance value at a wavelength of 455 nm. The N<sub>2</sub>H<sub>4</sub> concentration is calibrated by measuring the absorbance values of a series of standard N<sub>2</sub>H<sub>4</sub>·H<sub>2</sub>O solutions (**Fig. S8**).

***<sup>15</sup>N<sub>2</sub> Isotope Labeling Experiments.*** An isotopic labeling experiment utilized N-15 enriched gas (98% <sup>15</sup>N<sub>2</sub>) as the isotopic N<sub>2</sub> source to verify the nitrogen source in ammonia. The flow rate of the <sup>15</sup>N<sub>2</sub> gas during the experiment was adjusted to 5 mL min<sup>-1</sup> according to the literature. After NRR for 10 h, the acquired nitrogen species in the electrolyte was identified by <sup>1</sup>H (nuclear magnetic resonance, 400 MHz) NMR spectrometer.<sup>8</sup>

**Table S1.** The elemental composition and binding states based on the XPS spectra of the pristine CC, CC-APS 200, CC-APS 400, CC-APS 600, and CC-APS 800.

	<b>S/C at%</b>	<b>N/C at%</b>	<b>pyridinic N/total N %</b>	<b>pyrrolic N/total N %</b>	<b>graphitic N/total N %</b>
<b>Pristine CC</b>	0.00	1.77	40.78	23.21	36.01
<b>CC-APS 200</b>	0.61	3.59	41.47	33.42	25.10
<b>CC-APS 400</b>	0.93	7.42	19.10	51.34	29.56
<b>CC-APS 600</b>	1.45	8.31	35.76	35.98	28.26
<b>CC-APS 800</b>	2.51	8.23	24.97	39.02	36.01



**Table S2.** Comparison of N<sub>2</sub> electroreduction performance for CC-APS 800 with other carbon-based electrocatalysts under ambient conditions.

Catalyst	Electrolyte	NH <sub>3</sub> yield	FE %	Potential vs. RHE	References
CC-APS 800	0.2 M Na <sub>2</sub> SO <sub>4</sub> + 0.05 M H <sub>2</sub> SO <sub>4</sub>	<b>9.87×10<sup>-10</sup> mol</b> <b>s<sup>-1</sup> cm<sup>-2</sup></b>	<b>8.11</b>	<b>-0.3</b>	<b>This work</b>
N, P-codoped porous carbon	0.1 M HCl	1.08 μg h <sup>-1</sup> mg <sub>cat.</sub> <sup>-1</sup>	0.075	-0.1	ACS Appl. Mater. Interfaces. 2019,13,12408
Fe <sub>2</sub> O <sub>3</sub> -CNTs	2 M KHCO <sub>3</sub>	3.50×10 <sup>-12</sup> mol s <sup>-1</sup> cm <sup>-2</sup>	0.15	-2.0	Angew. Chem. Int. Ed. 2017, 56, 2699.
MoS <sub>2</sub> /CC	0.1 M Na <sub>2</sub> SO <sub>4</sub>	8.08×10 <sup>-11</sup> mol s <sup>-1</sup> cm <sup>-2</sup>	1.17	-0.2	Adv. Mater. 2018, 1800191.
commercial CC	0.1 M Na <sub>2</sub> SO <sub>4</sub> + 0.02 M H <sub>2</sub> SO <sub>4</sub>	5.6×10 <sup>-11</sup> mol s <sup>-1</sup> cm <sup>-2</sup>	1.29	-0.8	Chem. Commun. 2018,54,11188
VN/CC	0.1 M HCl	2.48×10 <sup>-10</sup> mol s <sup>-1</sup> cm <sup>-2</sup>	3.58	-0.3	Chem. Commun. 2018, 54, 5323.
defect-rich fluorographene	0.1 M Na <sub>2</sub> SO <sub>4</sub>	9.3 μg h <sup>-1</sup> mg <sub>cat.</sub> <sup>-1</sup>	4.2	-0.7	Chem. Commun. 2019,55,4266

nanosheet					
N, P co-doped porous carbon	0.1 M HCl	0.97 $\mu\text{g h}^{-1}$ $\text{mg}_{\text{cat.}}^{-1}$	4.2	-0.2	Chem. Commun. 2019,55,687
amorphous O-doped carbon nanosheet	0.1 M HCl	20.15 $\mu\text{g h}^{-1}$ $\text{mg}_{\text{cat.}}^{-1}$	4.97	-0.6	Chemistry A European Journal 2019,25,1914
N doped porous carbon	1.0 M HCl	$1.31 \times 10^{-10}$ mol $\text{s}^{-1} \text{cm}^{-2}$	5.2	-0.3	Angew. Chem. Int. Ed. 2018, 57, 1.
Nitrogen-free commercial carbon cloth with rich defects	0.1 M $\text{Na}_2\text{SO}_4$ + 0.02 M $\text{H}_2\text{SO}_4$	$2.59 \times 10^{-10}$ mol $\text{s}^{-1}$ $\text{cm}^{-2}$	6.92	-0.3	Chem. Commun. 2018,54,11188
Sulfur dots–graphene nanohybrid	0.5 M $\text{LiClO}_4$	28.56 $\mu\text{g h}^{-1}$ $\text{mg}_{\text{cat.}}^{-1}$	7.07	-0.85	Chem. Commun. 2019,55,3152
Boron-Doped Graphene	0.05 M $\text{H}_2\text{SO}_4$	$1.6 \times 10^{-10}$ mol $\text{s}^{-1}$ $\text{cm}^{-2}$	10.8	-0.5	Joule 2018,8,1610
B-N Pairs Enriched Defective Carbon Nanosheets	0.1 M HCl	7.75 $\mu\text{g h}^{-1}$ $\text{mg}_{\text{cat.}}^{-1}$	13.79	-0.3	Small 2019,15,e1805029

**Table S3.** The elemental contents and binding states calculated from the corresponding XPS spectra on CC-APS 800 before and after two times durability test.

	<b>S/C</b>	<b>N/C</b>	<b>pyridinic</b>	<b>pyrrolic</b>	<b>pyridinic and</b>	<b>graphitic</b>
	<b>at%</b>	<b>at%</b>	<b>N: total N</b>	<b>N: total N</b>	<b>pyrrolic N:</b>	<b>N: total N</b>
			<b>%</b>	<b>%</b>	<b>total N %</b>	<b>%</b>
<b>new-made CC-APS 800</b>	2.51	8.23	24.97	39.02	63.99	36.01
<b>CC-APS 800 after two times durability test</b>	2.64	8.49	54.23	14.16	68.39	31.61

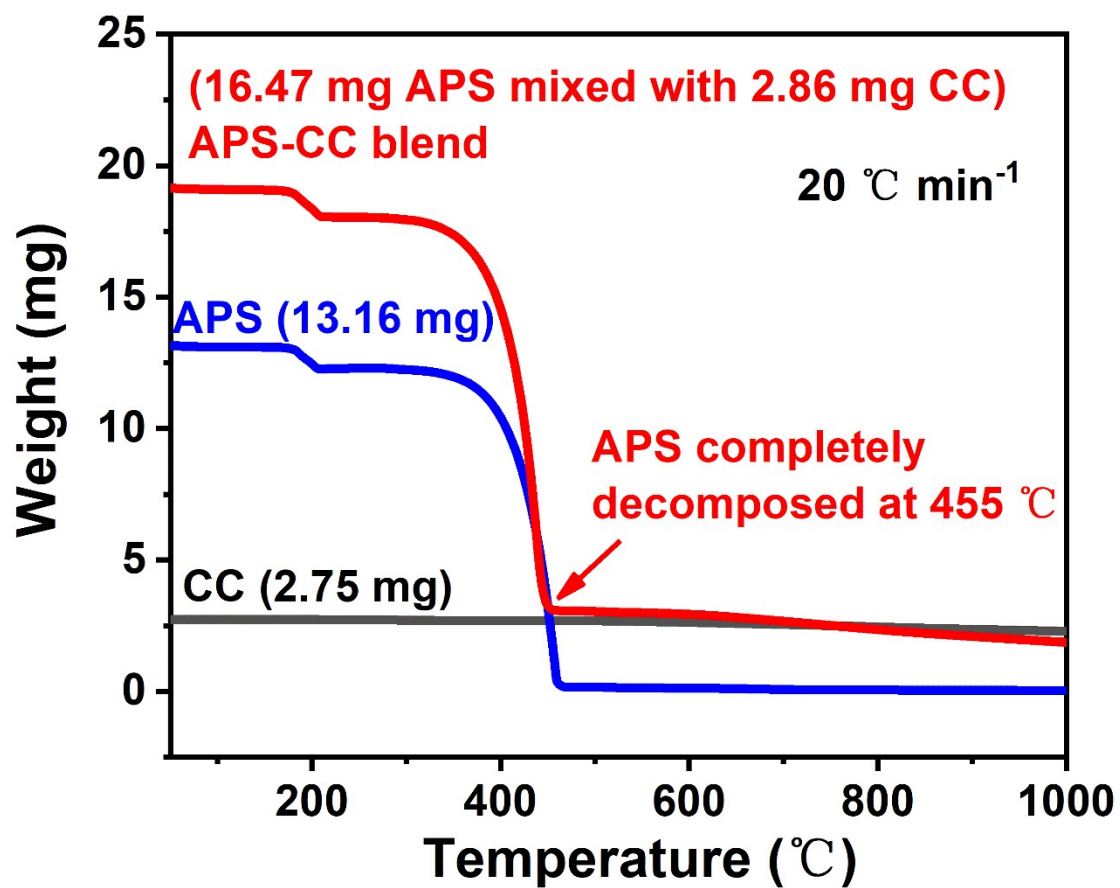


**Fig. S1.** TGA curves of carbon cloth (CC), ammonia persulfate (APS), and APS-CC blend in the N<sub>2</sub> atmosphere with a heating rate of 20 °C s<sup>-1</sup>.

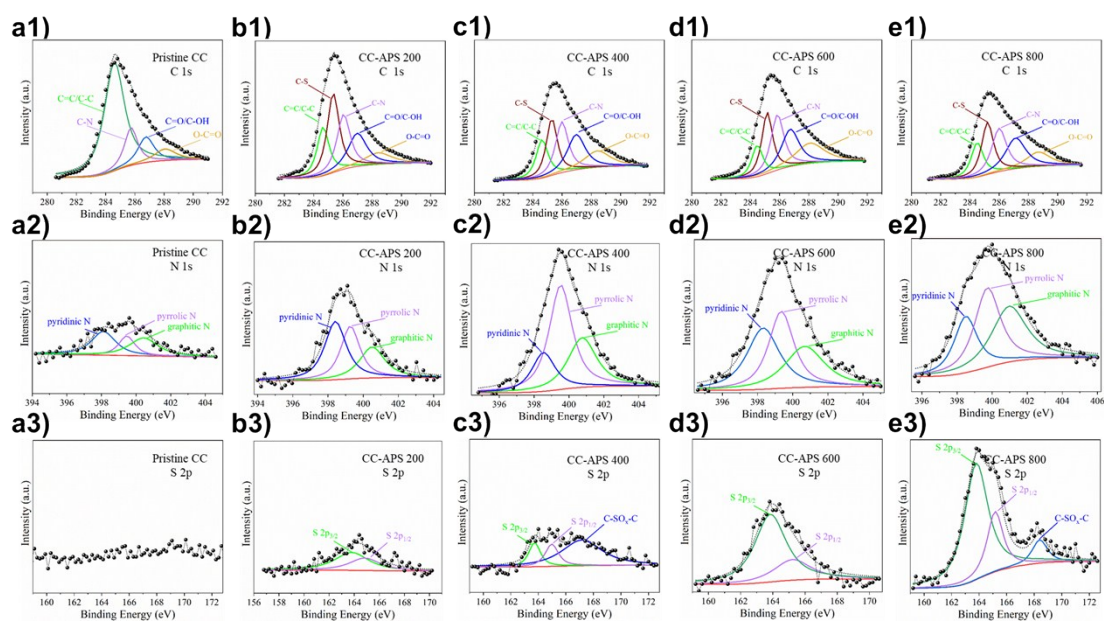


**Fig. S2.** XPS spectra of C 1s, N 1s and S 2p of (a1~a3) the pristine CC, (b1~b3) CC-APS 200, (c1~c3) CC-APS 400, (d1~d3) CC-APS 600, and (e1~e3) CC-APS 800.

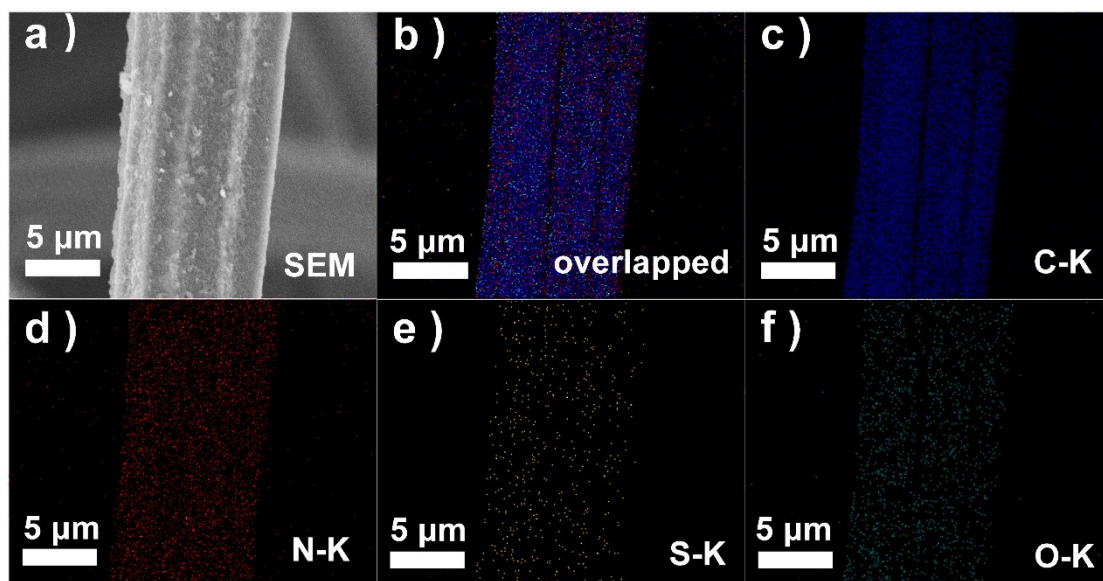


**Fig. S3.** (a) SEM of CC-APS 800. EDS images of CC-APS 800: (b) the overlapped image, (c) C-K, (d) N-K, (e) S-K, and (f) O-K.

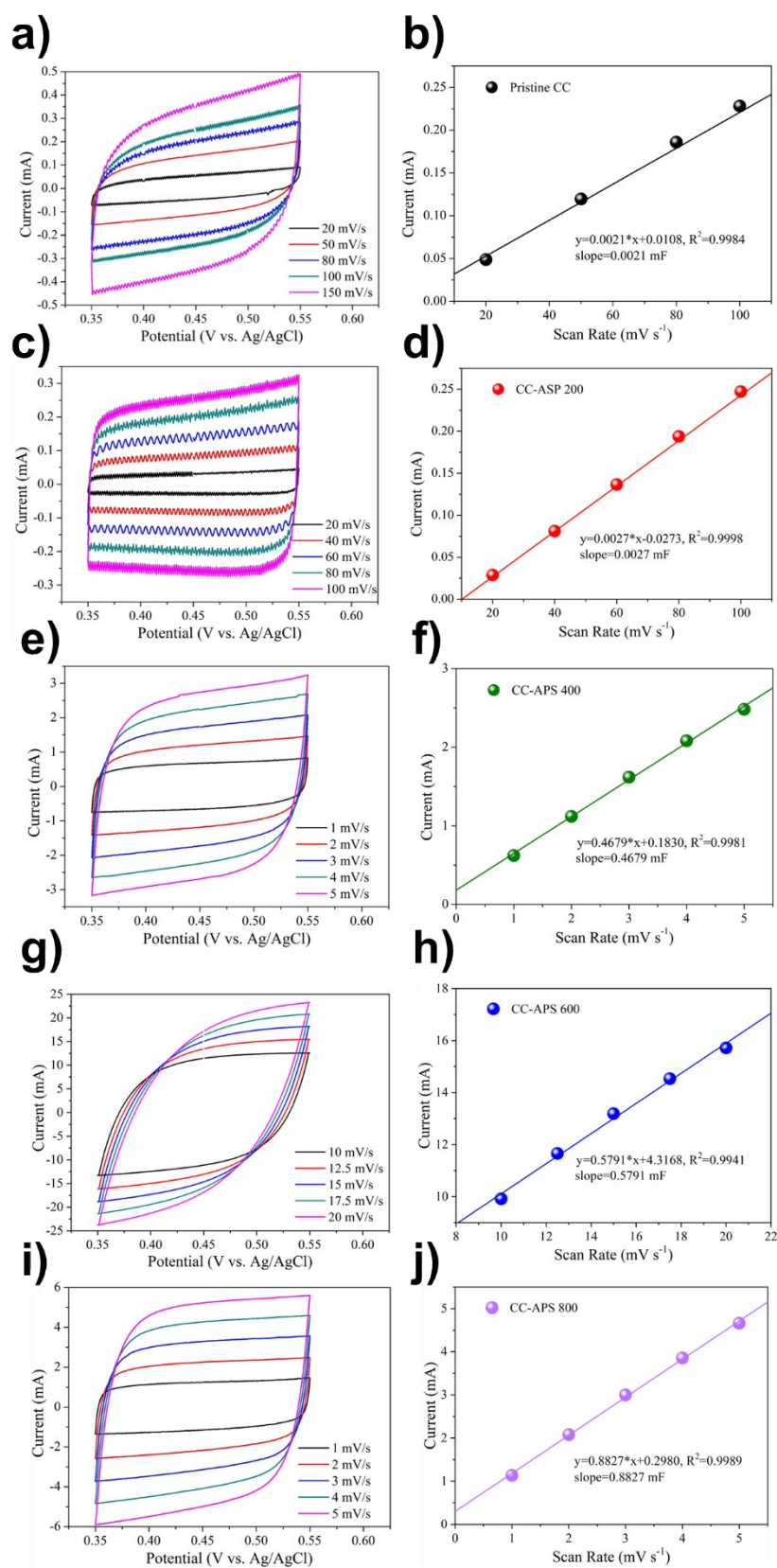


**Fig. S4.** CV curves with different scan rates and the fitting lines of the double electric

layer capacities in (a, b) the pristine CC, (c, d) CC-APS 200, (e, f) CC-APS 400, (g, h) CC-APS 600, and (i, j) CC-APS 800. With the same area of  $0.5 \text{ cm}^2$ , the calculated ECSA of the pristine CC, CC-APS 200, CC-APS 400, CC-APS 600, and CC-APS 800 is 0.0021, 0.0027, 0.4679, 0.5791 and 0.8827 mF, respectively.



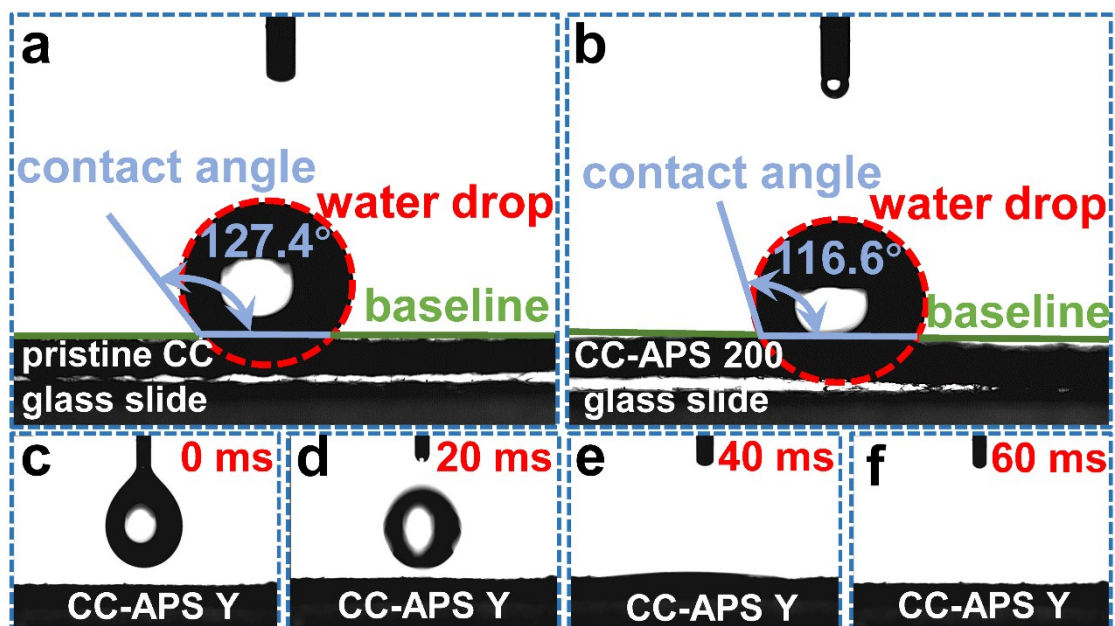


**Fig. S5.** Photographs of the contact angels on (a) the pristine CC and (b) CC-APS 200. (c-f) Photographs of the water droplet on CC-APS Y (Y=400, 600, or 800) at different falling times (c=0 ms, d=20 ms, e=40 ms, and f=60 ms). The contact angle appears as  $\sim 0^\circ$  at the moment of the contact, indicating the super-hydrophilic property of the surface of CC-APS Y.

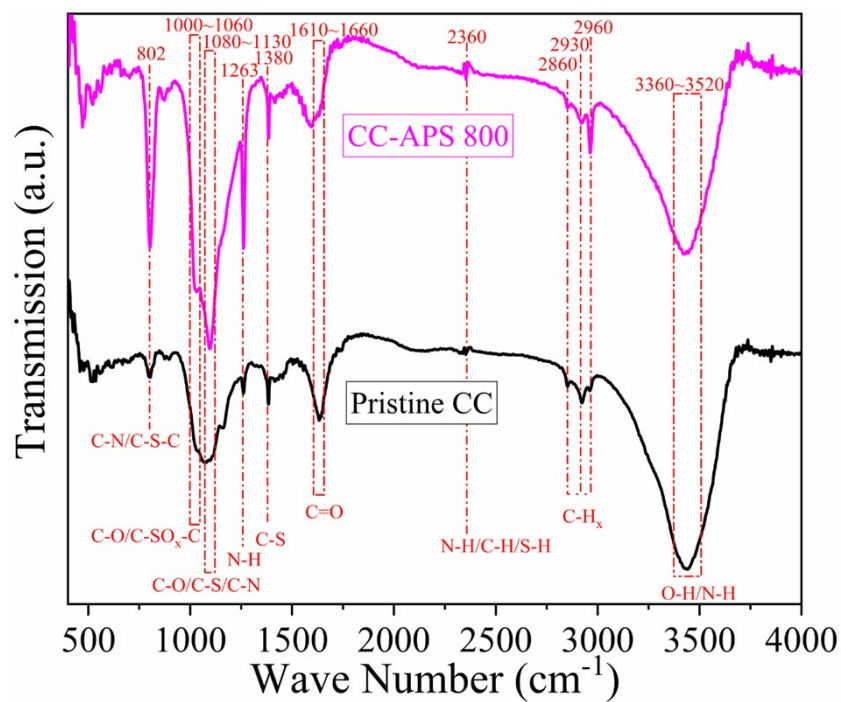


**Fig. S6.** FTIR spectra of the pristine CC and the CC-APS 800. The enhanced absorption at 802, 1000~1060, 1080~1130, 1263, and 1380  $\text{cm}^{-1}$  in CC-APS 800 mainly corresponds to several S- and N-containing groups as marked in the figure.

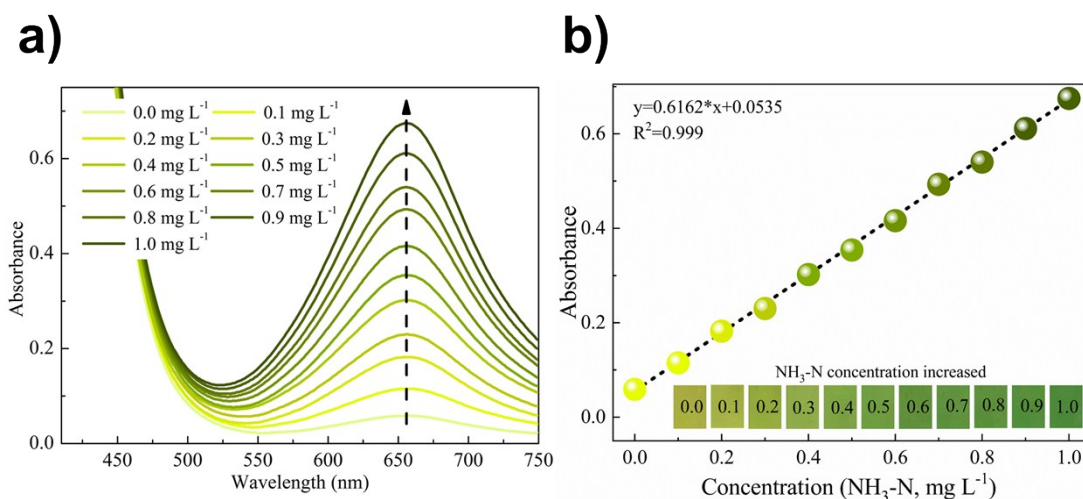


**Fig. S7.** (a) The UV-vis absorption spectra of standard  $(\text{NH}_4)_2\text{SO}_4$  solution with various concentration (0.0, 0.1, 0.2, 0.3, 0.4, 0.5, 0.6, 0.7, 0.8, 0.9 and 1.0  $\text{mg NH}_3\text{-N L}^{-1}$ ) after incubation for 2 h under room temperature. (b) The fitted regression line based on the values of absorption at 655 nm for the calculation of  $\text{NH}_3\text{-N}$  concentration.

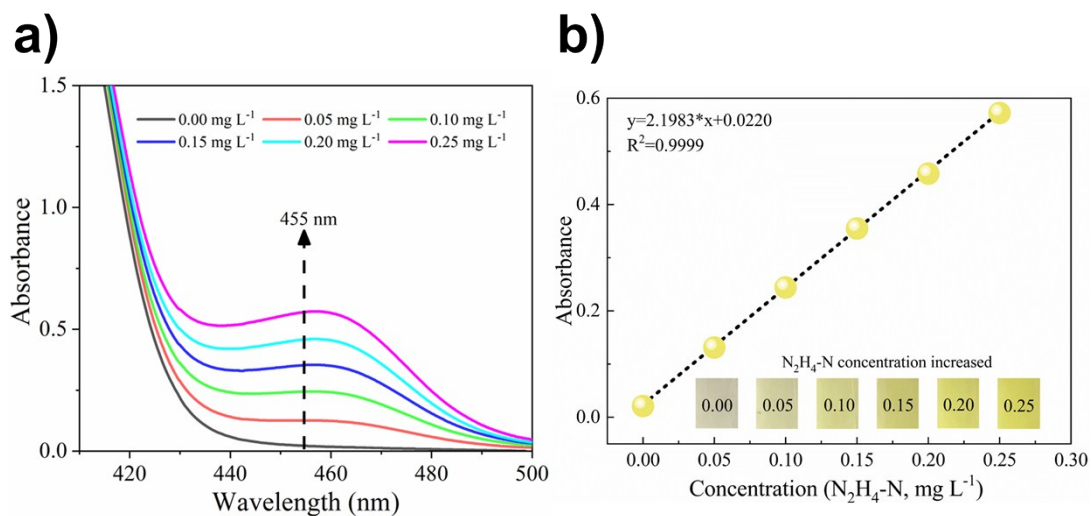


**Fig. S8.** (a) The UV-vis absorption spectra of standard  $N_2H_4$  solution with various concentration (0.00, 0.05, 0.10, 0.15, 0.02, and 0.25  $mg L^{-1}$ ) after incubation for 20 min under room temperature. (b) The fitted regression line based on the values of absorption at 455 nm for the calculation of  $N_2H_4$  concentration.

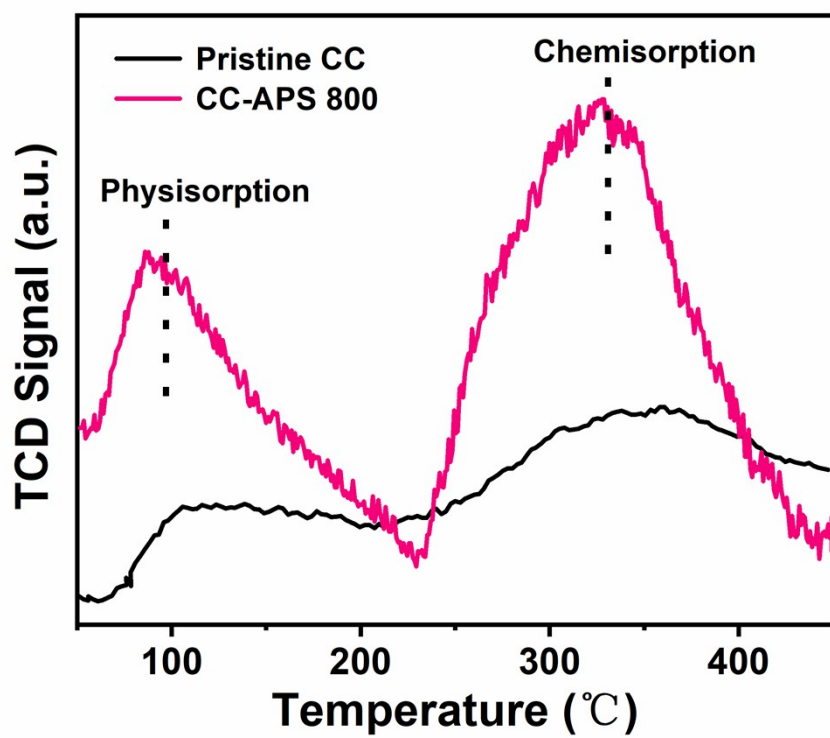


**Fig. S9.** N<sub>2</sub> TPD curves of pristine CC and CC-APS 800.

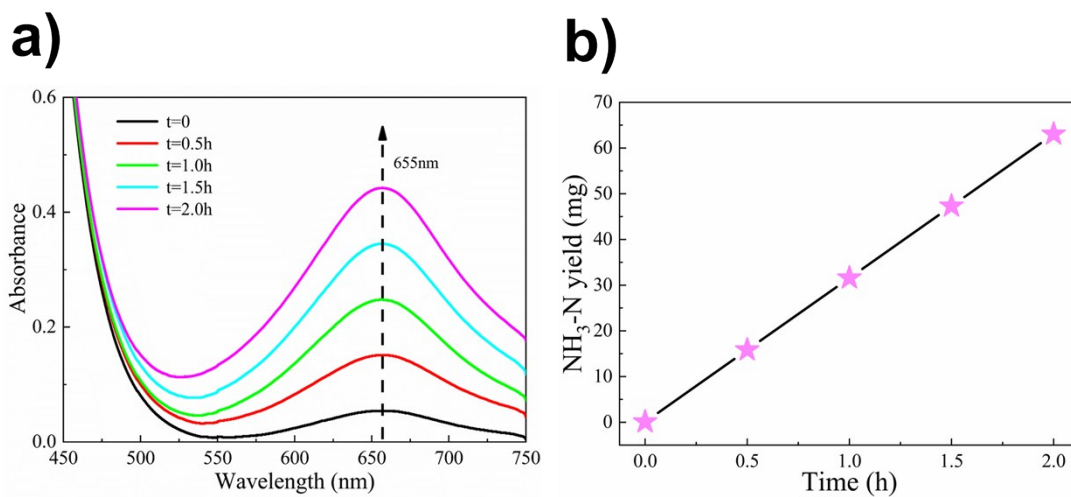


**Fig. S10.** (a) UV-vis spectra of N<sub>2</sub>-saturated 0.05 M H<sub>2</sub>SO<sub>4</sub> electrolyte stained with indophenol indicator and (b) NH<sub>3</sub> yielding after NRR test for different reaction times at -0.3 V vs. RHE using CC-APS 800.

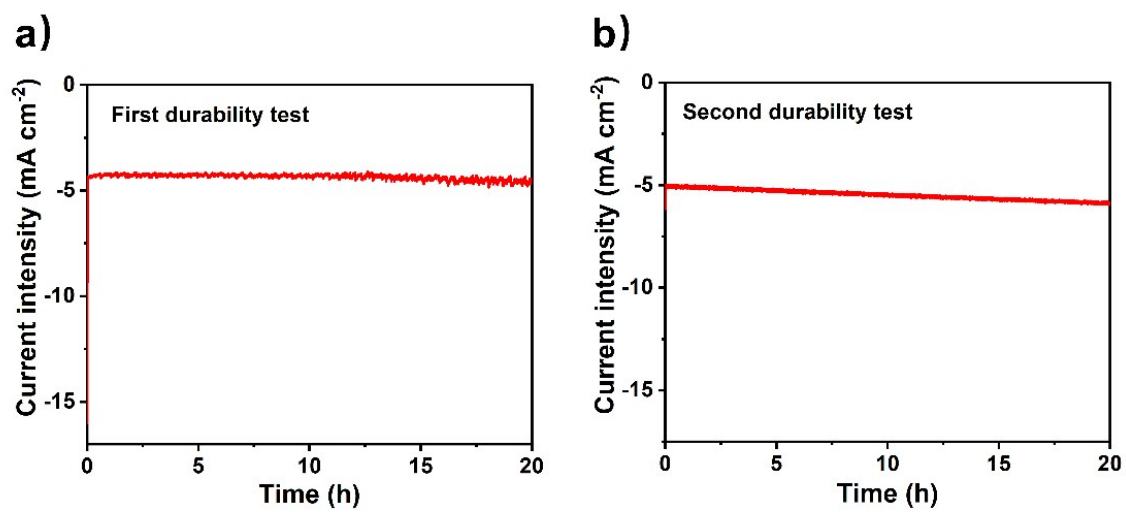


**Fig. S11.** The current density of CC-APS 800 during two times durability tests in N<sub>2</sub> saturated 0.05 M H<sub>2</sub>SO<sub>4</sub> electrolyte at -0.3 V vs. RHE. (a) First durability test. (b) Second durability test.

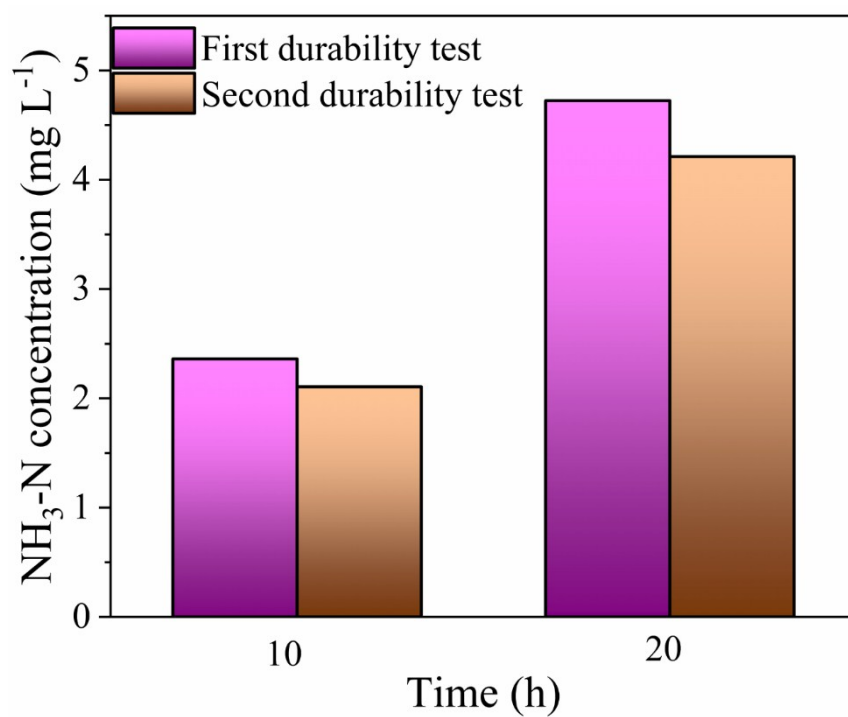


**Fig. S12.** The ammonia yielding of CC-APS 800 during two times durability tests (20 h for each test) in  $\text{N}_2$  saturated 0.05 M  $\text{H}_2\text{SO}_4$  electrolyte at -0.3 V vs. RHE.



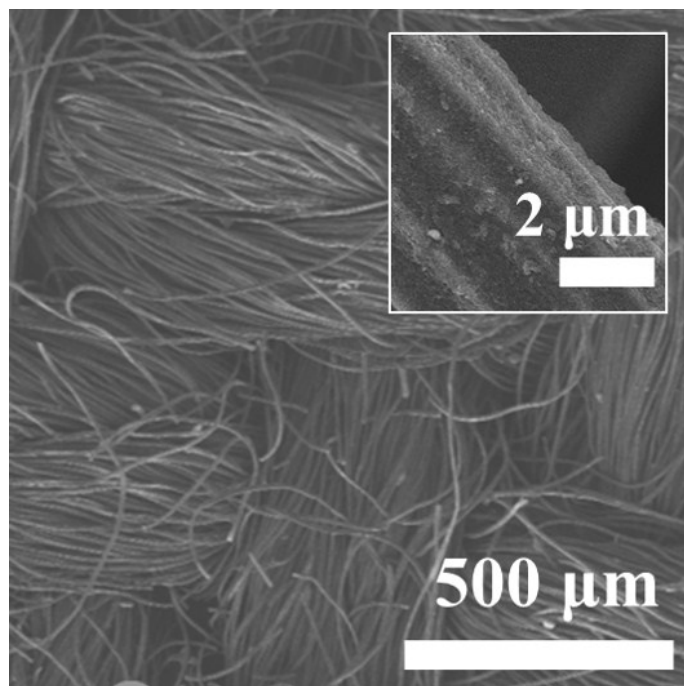


**Fig. S13.** The SEM image of CC-APS 800 after two times durability tests (a total electrolysis time of 40 h) in N<sub>2</sub> saturated 0.05 M H<sub>2</sub>SO<sub>4</sub> electrolyte at -0.3 V vs. RHE.

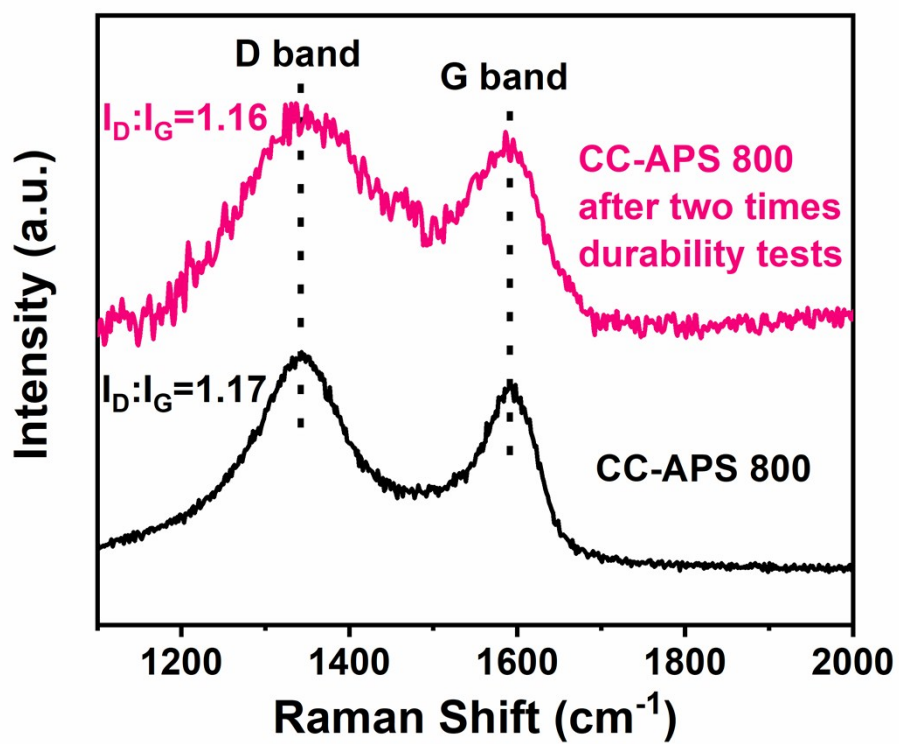


**Fig. S14.** Raman spectra of CC-APS 800 before and after two times durability tests (a total electrolysis time of 40 h) in N<sub>2</sub> saturated 0.05 M H<sub>2</sub>SO<sub>4</sub> electrolyte at -0.3 V vs. RHE.

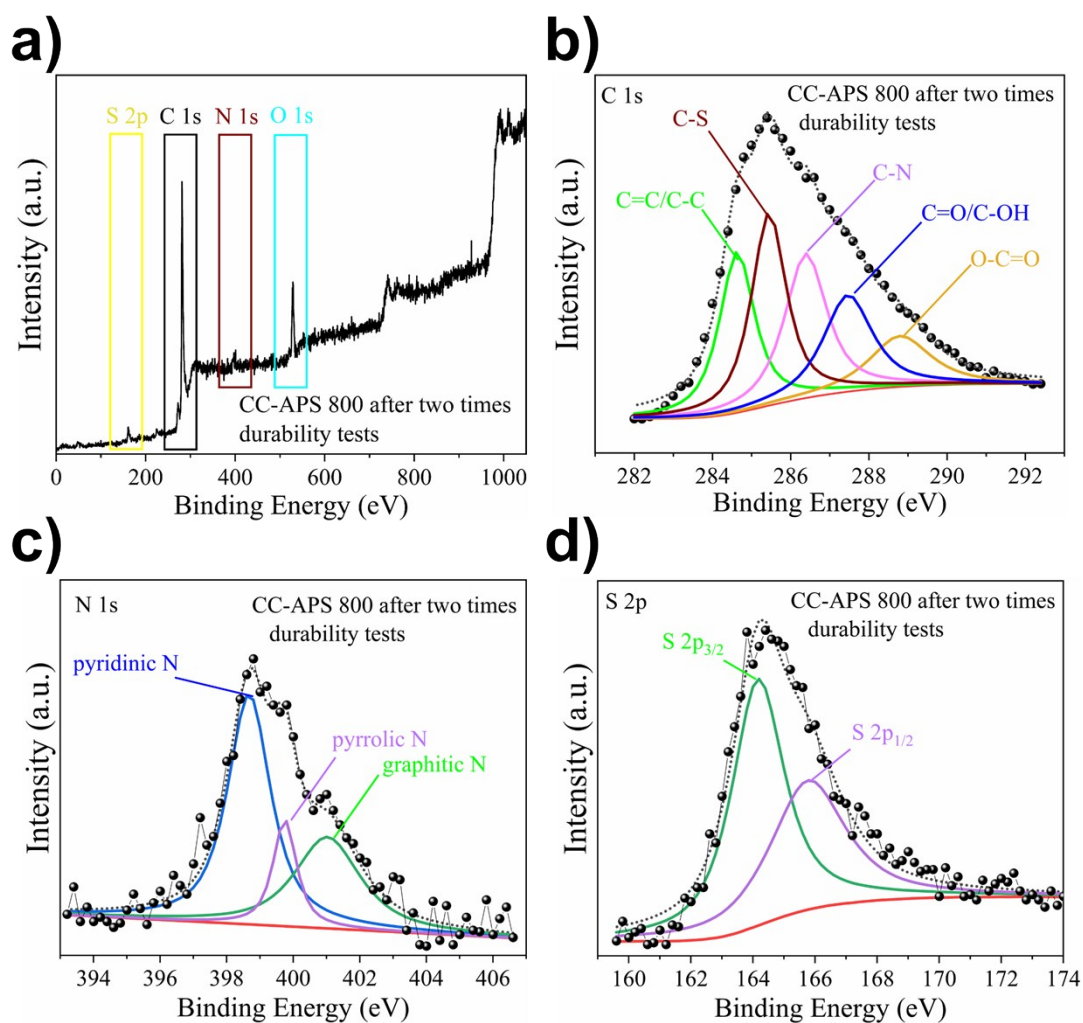


**Fig. S15.** (a) XPS overall spectrum and high-resolution XPS spectra of (b) C 1s, (c) N 1s, and (d) S 2p of CC-APS 800 after two times durability tests (a total electrolysis time of 40 h) in N<sub>2</sub> saturated 0.05 M H<sub>2</sub>SO<sub>4</sub> electrolyte at -0.3 V vs. RHE.

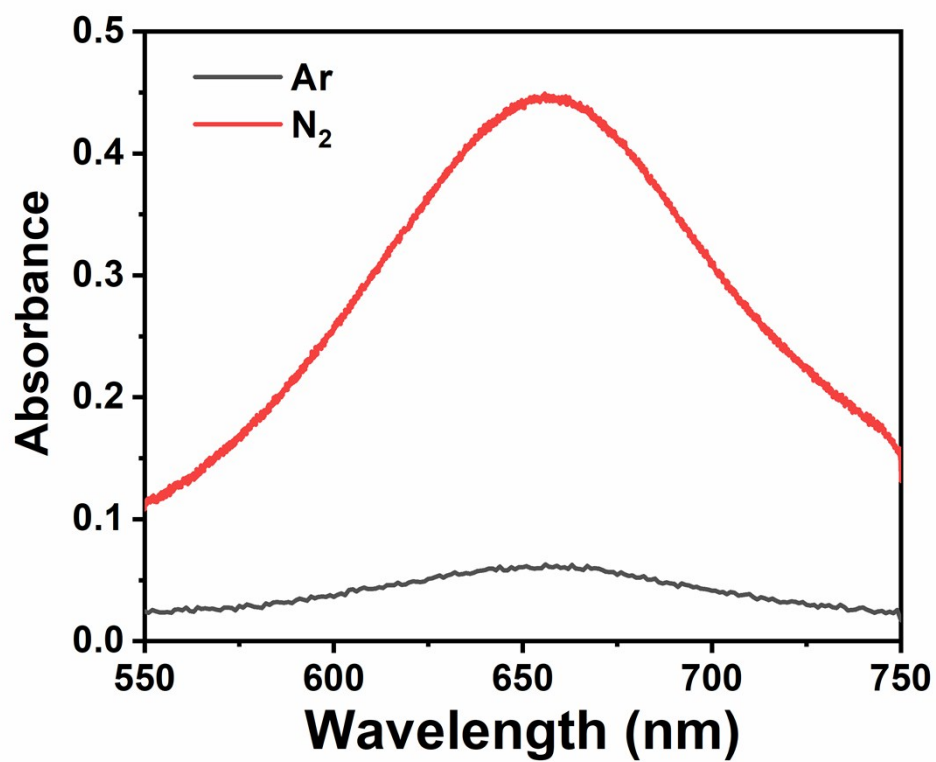


**Fig. S16.** The UV-vis absorption spectra at -0.3 V vs. RHE in 100 mL 0.05 M H<sub>2</sub>SO<sub>4</sub> electrolyte bubbled with Ar and N<sub>2</sub>. (NH<sub>3</sub>).

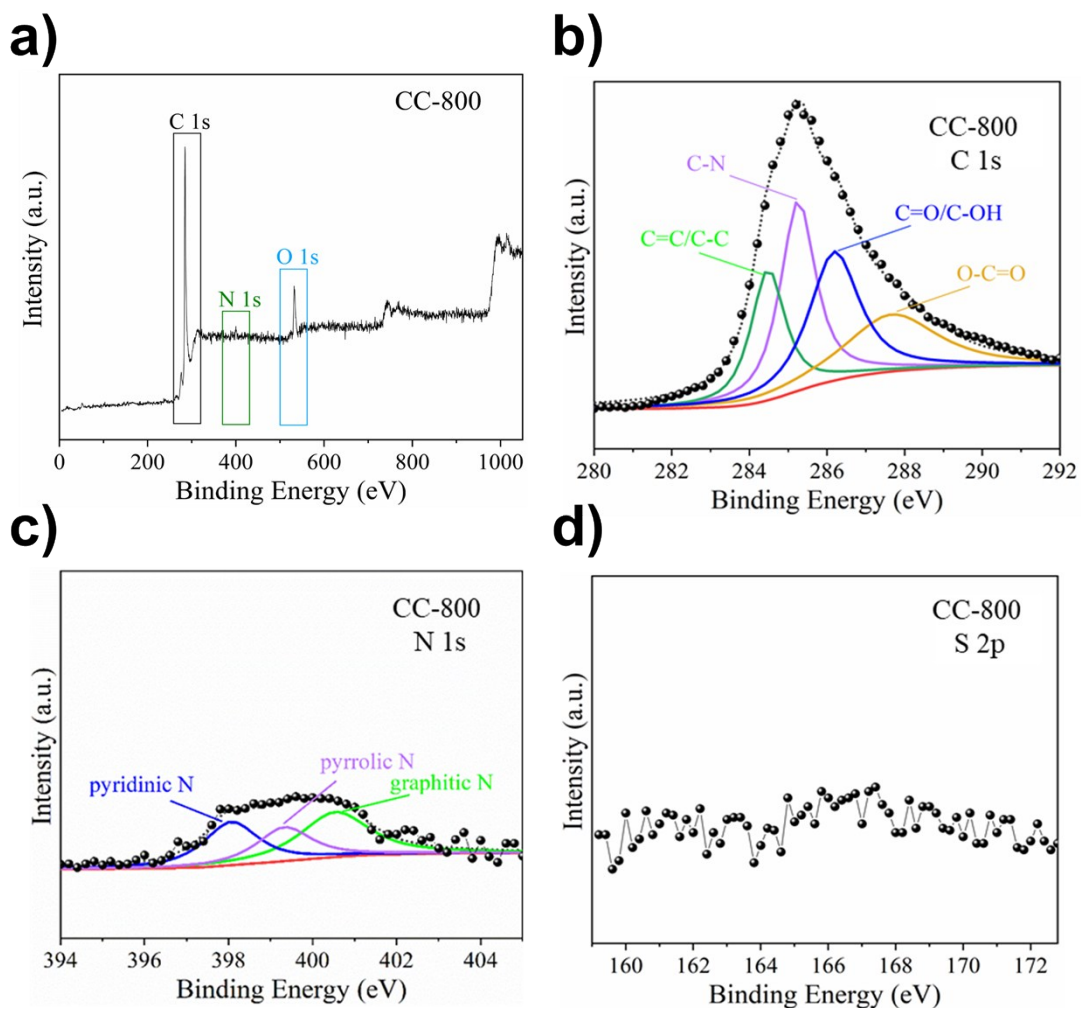


**Fig. S17.** (a) XPS overall spectra of CC 800. High-resolution XPS spectra of (b) C 1s, (c) N 1s, and (d) S 2p of CC 800.

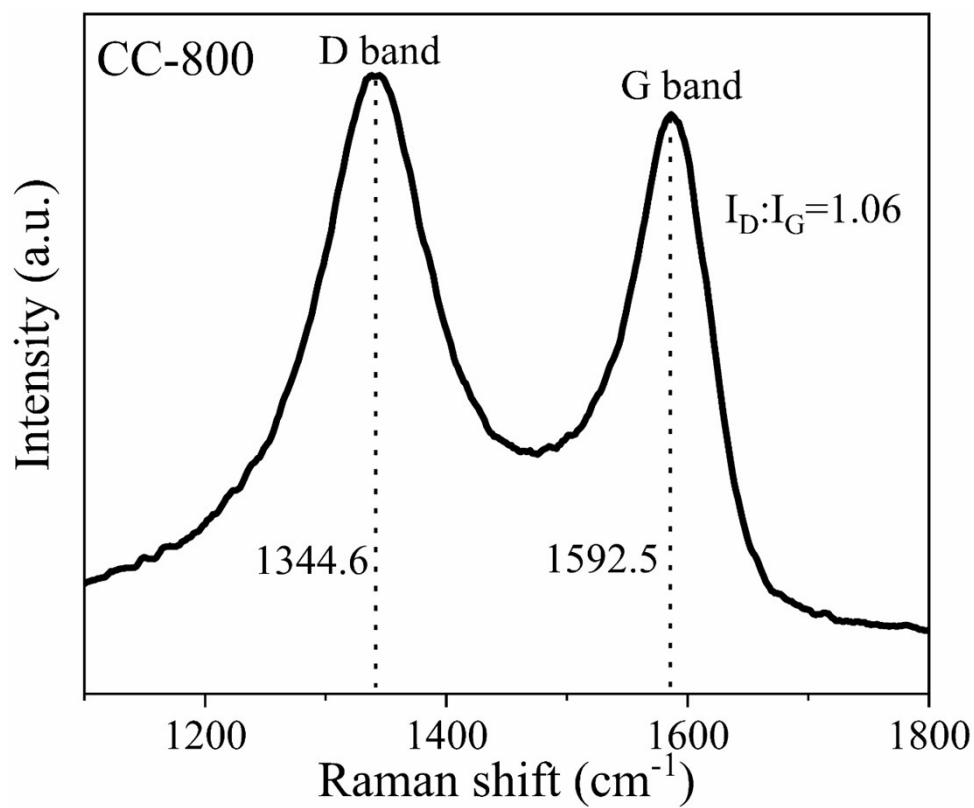


**Fig. S18.** Raman spectrum of CC-800.

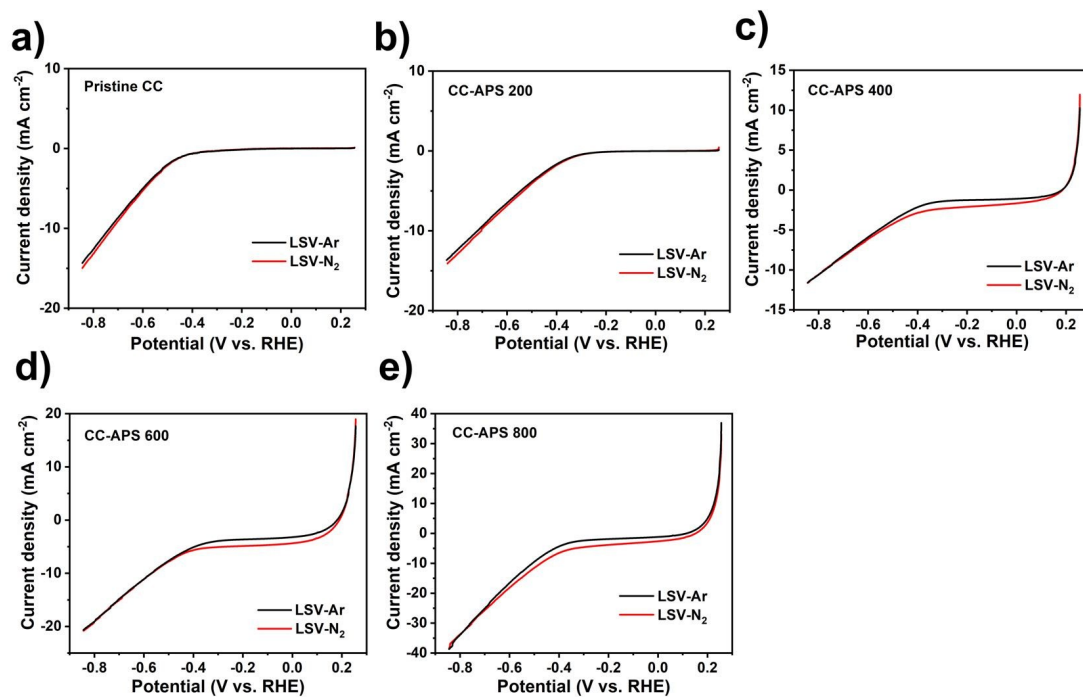


**Fig. S19.** LSV curves from 0.25 V to -0.85 V vs. RHE in (a) the pristine CC, (b) CC-APS 200, (c) CC-APS 400, (d) CC-APS 600, and (e) CC-APS 800 in the Ar or N<sub>2</sub> saturated electrolyte of 0.05 M H<sub>2</sub>SO<sub>4</sub> with a scanning rate of 5 mV s<sup>-1</sup>.

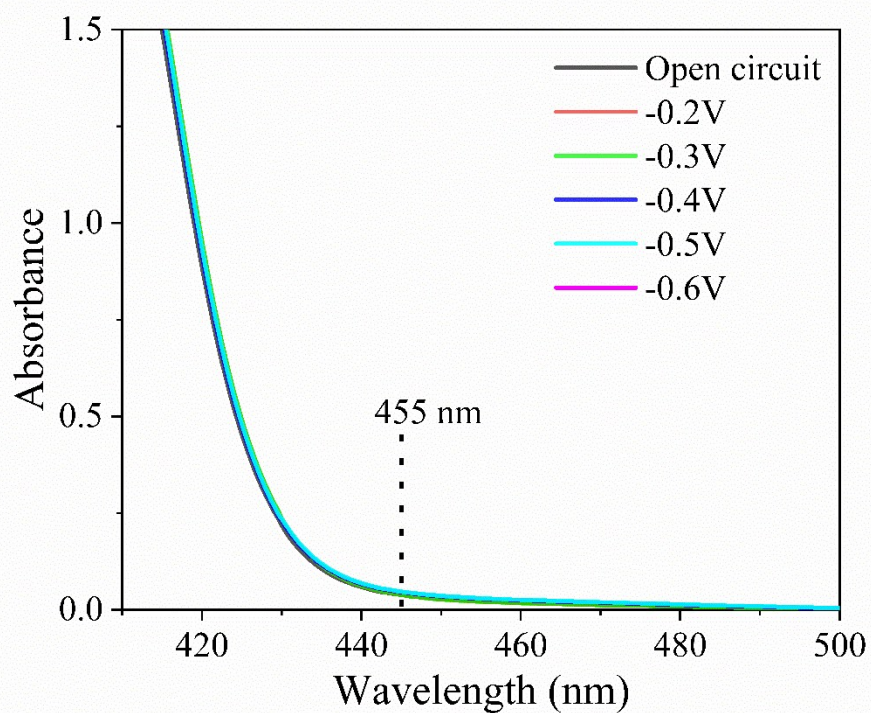


**Fig. S20.** The UV-vis spectra of the 0.05 M H<sub>2</sub>SO<sub>4</sub> electrolyte after electrolysis with CC-APS 800 under various potentials for 2 h as chromogenically stained *via* the Watt method.



## Reference

1. C. Tang and S. Z. Qiao, *Chem Soc Rev*, 2019, **48**, 3166-3180.
2. C. Tang and S. Z. Qiao, *Joule*, 2019, **3**, 1573-1575.
3. L. Zhang, X. Ji, X. Ren, Y. Ma, X. Shi, Z. Tian, A. M. Asiri, L. Chen, B. Tang and X. Sun, *Advanced Materials*, 2018, **30**, 1800191.
4. Y. M. Liu, Y. Su, X. Quan, X. F. Fan, S. Chen, H. T. Yu, H. M. Zhao, Y. B. Zhang and J. J. Zhao, *ACS Catal.*, 2018, **8**, 1186-1191.
5. C. Chen, D. F. Yan, Y. Wang, Y. Y. Zhou, Y. Q. Zou, Y. F. Li and S. Y. Wang, *e*, 2019, **15**, 1805029.
6. X. Zhang, M. M. Han, G. Q. Liu, G. Z. Wang, Y. X. Zhang, H. M. Zhang and H. J. Zhao, *Appl. Catal. B-Environ.*, 2019, **244**, 899-908.
7. L. Q. Li, C. Tang, D. Z. Yao, Y. Zheng and S. Z. Qiao, *ACS Energy Lett.*, 2019, **4**, 2111-2116.
8. S. Z. Andersen, V. Čolić, S. Yang, J. A. Schwalbe, A. C. Nielander, J. M. McEnaney, K. Enemark-Rasmussen, J. G. Baker, A. R. Singh and B. A. Rohr, *Nature*, 2019, **570**, 504-508.